DOI:10.14753/SE.2025.3097

SEMMELWEIS EGYETEM

DOKTORI ISKOLA

Ph.D. értekezések

3097.

KESZTYŰS ARTÚR JÓZSEF

Krónikus betegségek gyermekkori prevenciója

című program

Programvezető: Dr. Szabó Attila, egyetemi tanár

Témavezető: Dr. Nagy Krisztián, egyetemi docens

DOI:10.14753/SE.2025.3097

Optimization and novel application of Cone Beam CT in the treatment of patients with orofacial clefts

PhD thesis

Dr. Artúr József Kesztyűs

Károly Rácz Doctoral School of Clinical Medicine

Semmelweis University

Supervisor: Krisztián Nagy, MD, Ph.D., D.Sc

Official reviewers: Zsuzsanna Gurdán, MD, Ph.D

Dávid Ledvai, MD, Ph.D

Head of the Complex Examination Committee: Alán Alpár, MD, Ph.D.

Members of the Complex Examination Committee: István Berkes, MD, Ph.D.

Tamás Huszár, MD, Ph.D.

Budapest

2024

DOI:10.14753/SE.2025.3097

Table of Contents

DOI:10.14753/SE.2025.3097

DOI:10.14753/SE.2025.3097

List of Abbreviations

2D: two-dimensional
3D: three-dimensional
AL: arch length
ALADA: as low as diagnostically acceptable
ALADAIP: as low as diagnostically acceptable being indication-oriented and patient-specific
ALARA: as low as reasonably achievable
ANOVA: one-way analysis of variance
ANS-PNS: anterior nasal spine–posterior nasal spine distance
BCLP: bilateral cleft lip and palate
CAD: computer-aided design
CBCT: cone-beam computed tomography
CF: bilateral maxillary first molar's central fossae distance
CL: cleft lip
CLA: cleft lip and alveolus
CLAP: cleft lip, alveolus, and palate
cm^2: square centimeter
CP: cleft palate
CT: Computed Tomography
CV: coefficient of variation
DAP: dose area product
DICOM: Digital Communications in Medicine
DIMITRA: Dentomaxillofacial paediatric imaging: an investigation towards low dose radiation induced risks
DVT: Dental Volumetric Tomography
FOV: Field of View
Jug: bilateral jugular distance
KN: Dr. Krisztián Nagy
kV: kilovolt

LOWESS: locally weighted scatterplot smoothing

mA: milliampere

mm: millimetre

mGy: milligray

MRI: magnetic resonance imaging

MSCT: multi slice computed tomography

OHIP-14: Oral Health Impact Profile

OHQoL: modified Health Related Quality of Life Measure

OHQoL: Health Related Quality of Life Measure

PABG: primary alveolar bone grafting

PACS/AFGA: picture archiving and communication system

PCEJ: bilateral palatal cementoenamel junction distance

PVD: palatal vault depth

SABG: secondary alveolar bone grafting

SADS: Social Avoidance and Distress Scale

SEM: standard error of the mean

STL: standard tessellation language

TAGB: tertiary alveolar bone grafting

UCLP: unilateral cleft lip and palate

VCEJ: bilateral vestibular CEJ distance

VFS: Videofluoroscopy

VPD: velopharyngeal dysfunction

VPI: velopharyngeal insufficiency

DOI:10.14753/SE.2025.3097

1. Introduction:

1.2. Etiology, incidence, and clinical appearance of patients with orofacial clefts

Orofacial clefts are one of the most common congenital anomalies in the craniofacial region, with an incidence rate of 1 per 500-700 births (1). It is considered a multifactorial condition associated with genetic and environmental etiological factors (2). Cleft patients can be divided according to the affected structures: cleft lip (CL), cleft lip and alveolus (CLA), cleft palate (CP), cleft lip, alveolus, and palate (CLAP) and based on the site of the defect: unilateral or bilateral (3).

The condition results in esthetic and functional problems for the patients (Figure 1.) e.g. presence of oronasal fistula, collapsed maxillary dimensions, facial asymmetry, unsupported adjacent teeth, malocclusion and speech disorders (4) (5).

Nearly 20% of patients present with supernumerary teeth, and 50% with hypodontia (6) (7). Several studies reported delayed dental development of cleft patients when compared to non-cleft pediatric patients of the same age (8) (9).

In approximately 75% of the cases, an alveolar cleft is present as well (10). The disturbed development of the maxilla results in collapsed alveolar segments and decreased maxillary dimensions.

Generally, patients with clefts undergo several surgical and non-surgical interventions following an extensive treatment plan which is determined by a multidisciplinary team, including oral surgeons, orthodontists, plastic surgeons, and speech therapists (11) (12) (13). In most of the cases, patients are treated from infancy until the late teenage years.

If bony defects are present, alveolar bone grafting is an essential procedure in the treatment protocol (10). Restoring the integrity of the maxillary arch provides support for subsequent tooth eruption, adjacent teeth, and the nasal base (14) (15) (16) (17).

DOI:10.14753/SE.2025.3097

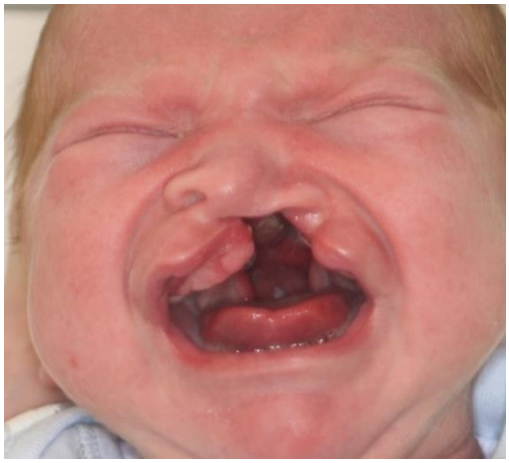

Figure 1. - Clinical appearance of a patient with cleft lip, palate, and alveolus (CLAP) – courtesy of Dr. Krisztián Nagy

1.2. Surgical treatment of patients with orofacial clefts

Management of complex soft and hard tissue deficiencies is a challenging task and is generally carried out in a staged approach. The interventions are performed at different ages of patients and aim to restore the integrity of the lip, soft palate, hard palate, and alveolus (18) (19). There are alterations among the different cleft centers regarding the exact timing, sequence, and technique of the interventions (20) (21).

Table 1. shows the treatment protocol for cleft patients at the Department of Pediatrics at Semmelweis University. The protocol has been established based on the Semmelweis cleft teams' experience and international recommendations (14) (22) (23) (24) (25). Primary surgical interventions are carried out regularly if a particular structure is involved (lip, palate, alveolar bone). Secondary surgeries are optional and depend on the patient's individual needs.

Table 1. - Treatment protocol for cleft patients at the Department of Pediatrics, Semmelweis University

Primary		Secondary	
Intervention	**Age**	**Intervention**	**Age**
Presurgical nasoalveolar molding (PNAM)	2-3 weeks	Pharyngoplasty	Individually
Surgical lip/nose adhesion	6-8 weeks	Rhinoplasty	Individually
Definite lip closure	4-6 months	Orthognathic surgery	Individually
Soft palate closure	9-12 months	Scar correction	Individually
Hard palate closure	2-4 years		
Alveolar cleft closure	8-10 years		

Alveolar bone augmentation is a crucial intervention in the treatment of patients with orofacial clefts. Most commonly it is categorized according to the timing of the intervention (26):

- Primary alveolar bone grafting (PABG): performed before the age of 2, after lip repair but prior to the repair of the palate.
- Secondary alveolar bone grafting (SABG): performed after the age of 2, in patients with mixed dentition.
- Tertiary alveolar bone grafting (TAGB): performed in patients with permanent dentition.

Until the 1970s primary alveolar bone grafting (PAGB) was the treatment of choice (27). However, long-term follow-up studies reported several drawbacks of the technique. Most prominently the adverse effect on maxillary growth and development (28).

Secondary alveolar bone grafting was introduced by Boyne and Sands in 1972 and has become the most common technique in the repair of bony cleft defects (14). It is optimally performed in the mixed dentition, between the age of 6-12 years (29) (30), providing support for the adjacent teeth and erupting canine (17). Closing the oronasal fistula and reconstructing the upper arch have favorable impact on the growth and development of the maxilla (16). Several studies confirmed that secondary alveolar bone grafting does not interfere with the growth and development of the maxilla (31) (32).

Majority of the cleft centers prefer autologous cancellous bone as a grafting material, the most common donor sites are: iliac crest, cranium, tibia, mandibular symphysis (33).

However, autologous bone remains the gold standard (34), in the literature several bone substitute materials have been described for alveolar bone grafting in cleft patients (allogenic, autologous, xenogeneic) (21) (35) (36).

The preferred technique at our center is cancellous bone from the anterior iliac crest, in a two-team approach.

Preoperative planning tools in cleft care, include study casts, clinical records, photography and clinical imaging. The latter is crucial in the diagnostic, presurgical and postoperative assessment (33), as visualization of the defect and the adjacent structures has a key role in establishing an individual treatment plan. The ideal imaging modality should be reproducible, easily accessible, non-invasive, and associated with minimal risk to the patient (37).

Imaging modalities in cleft care can be divided according to the type of tissues they provide information about.

1.3. Hard tissue imaging in patients with orofacial clefts

Hard tissues can be visualized using various imaging techniques, such as intraoral or panoramic radiographs, multi slice computed tomography (MSCT), and cone-beam computed tomography (CBCT). All the aforementioned imaging modalities rely on ionizing radiation; therefore the concern of radiation exposure has been raised early, especially when it comes to pediatric patients.

Historically the classification, treatment planning, and evaluation of CLAP patients was based on two-dimensional (2D) radiographs (38) (39) (40) (30). However, the resulting images do not provide spatial information, thus only linear measurements are possible. Additionally, there are several limitations due to distortion, positioning, superimposition, and magnification (41).

With the first introduction of Computed Tomography (CT) in the 1980s (42) (43), technological development enabled three-dimensional imaging. However, CT scans produce 200 to 300 times more radiation exposure than panoramic radiographs, therefore the justification of this imaging modality for patients with cleft has been a disputed question.

Later cone beam computed tomography (CBCT) /Dental Volumetric Tomography (DVT) was introduced which rapidly gained popularity due to its good contrast resolution, decreased radiation dose, lower costs and excellent ability to visualize bony structures of the head and neck region (44) (45) (46).

Recently CBCT has become the imaging modality of choice for a wide range of applications in the maxillofacial region (47), including CLAP patients. The use of three-dimensional (3D) imaging has been proven to increase predictability and reduce the operation time in cleft surgery (48). It provides high-quality images of the cleft dimensions and surrounding structures (e.g. presence, development and eruption status of adjacent teeth and possible connection with the nasal cavity).

Virtual planning can serve as an effective tool in the surgical management of clefts (49), by enabling the measurement of the needed bone graft. It can be applied for pre-operative virtual surgical planning (50) (51) (52) (53) (25), the evaluation of postoperative graft integration and volumetric assessment of the gained bone dimension (54) (52). In combination with 3D printing, the technique enables haptic evaluation of the preoperative site and the fabrication of surgical guides. Consequently, several guidelines and position papers recommend the use of cone beam CT imaging in cleft care (41).

Despite numerous clinical advantages that justify the application of 3D imaging in the pediatric population, the higher radiation dose remains a sensitive issue. Especially as cleft patients are generally treated for an extended period and undergo several radiological examinations throughout their lifetime. This can result in higher cumulative radiation exposure and associated risk (55) (56).

Various imaging recommendations have been introduced to optimize radiation doses, such as ALARA “as low as reasonably achievable” (ALARA) and ALADA “as low as diagnostically acceptable” (57) (58). The most recent guideline is ALADAIP “as low as diagnostically acceptable being indication-oriented and patient-specific”, published by Oenning et al (41). It suggests optimization by balancing image quality and radiation dose, while carefully selecting the indication of three-dimensional imaging (41). Optimization can also be achieved by the right timing and alteration of imaging modalities. In this regard, harmonization of imaging requirement by the different specializations involved in cleft care can be also considered as part of the strategy (59). In general, all recommendations emphasize justified cone-beam CT application and optimized imaging protocols in the pediatric population.

Most devices allow the modification of several acquisition parameters of CBCT units. Imaging recommendations in the pediatric field primarily suggested adjustments in tube voltage (kV), tube current (mA), and voxel size (60) (61). Additionally, several studies suggest the application of “low-dose” acquisition modes, which deliver clinically acceptable images using significantly lower radiation doses (62) (60).

Up until now, Field of View (FOV) has received less attention as a parameter in the optimization of CBCT acquisition. However, if patient specificity were applied more carefully it would allow reduced radiation dose without compromising image quality. The future evolution of modern CBCT devices will allow more options for individual FOV selection, thus Field Of View adjustment could serve as an important element in the optimization strategy, especially when it comes to children (41).

To apply patient-specific FOV settings in the pediatric population, maxillary dimensions need to be determined for the different age- and gender groups. Most studies in this field have assessed two-dimensional cephalometric radiographs and dental casts to describe the size and development of the dental arches (63) (64) (65) (66) (67) (68). The aforementioned limitations of 2D imaging methods such as superimposition, distortion, magnification, and errors by patient positioning do not allow the implementation of this data into three-dimensional FOV recommendations. Selected landmarks and measurements referred to skeletal and dental levels separately, however,

comprehensive information would be needed regarding the maxilla and the surrounding structures. To formulate recommendations for the optimal FOV selection, a normative dataset is needed rather than information on the development and growth patterns of the maxillary structures. Currently, to our knowledge, there are no studies assessing pediatric maxillary dimensions in age- and gender-specific groups, using CBCT imaging. This information is crucial to formulate age- and gender-specific FOV recommendations.

Today there are over 220 CBCT machines on the market (69), with a large variety of hardware and software options, resulting in a wide range of image quality and effective dose emissions (70). Comparison of different CBCT devices or imaging protocols for specific indications is very difficult as ethical considerations do not allow multiple scanning of a single patient only for optimization purposes, especially in the pediatric population.

It is well known that image quality is influenced by several factors, therefore varying the subject presents a challenge for optimization studies as these should be carried out under standardized and controlled circumstances.

Thus, for this task anthropomorphic phantoms are needed, which show similar radiological characteristics to patients. To achieve this goal, the artificial structures need to mimic the absorption and scattering characteristics of natural hard and soft tissues without creating artifacts. Publications in this field described different phantoms, using commercially available and custom-made versions (71) (72) (73) (74) (75) (76), one of the biggest challenges remained to achieve a realistic soft tissue appearance. Oenning et al described the development of the DIMITRA phantoms skulls (77), the first age-specific pediatric phantoms, using Mix-D as a soft tissue equivalent material (78). The phantoms have been validated for optimization studies using different CBCT units and protocols (62). However, to our knowledge, there are no age-specific pediatric anthropomorphic phantoms with orofacial clefts existing.

1.4. Soft tissue imaging in patients with orofacial clefts

A common clinical question in cleft care is the presence of velopharyngeal insufficiency (VPI) also known as velopharyngeal dysfunction (VPD). Normally, the coordinated movement of the velopharyngeal muscles results in the separation of the nasal and oral cavities. This function is crucial for adequate speech and swallowing. The condition is commonly present in cleft patients due to the congenital anatomical irregularity of the soft palate. Phonation deficiencies include hypernasality, nasal turbulence, and decreased vocal intensity (79).

Diagnostic evaluation of VPI is generally carried out by a multidisciplinary team consisting of speech therapists, radiologists, and surgeons (80). In addition to patient history, clinical examination, and speech assessment, imaging has a crucial role in the diagnosis and treatment decision-making. It can provide objective information regarding the movement of the soft palate during speech tasks (81) (82) (83).

The velopharyngeal function can be evaluated using various imaging techniques, such as flexible nasopharyngoscopy, video fluoroscopy, multiview fluoroscopy, and dynamic magnetic resonance (MRI) (84) (85). All imaging techniques allow the visualization of the velopharyngeal structures but have limitations as well.

Flexible nasopharngoscopy (or fiberoptic nasoendoscopy) allows a direct view of the velopharyngeal structures during speech. Although it is a widely used diagnostic method (86), it requires a well-cooperating patient, as it is an inconvenient and invasive technique.

Videofluoroscopy (VFS) and multiview fluoroscopy are common, non-invasive diagnostic tools in the diagnosis of VPI (87). Images can be taken in frontal and lateral views to evaluate the valving function of the velopharynx. However the method is associated with ionizing radiation, which is a concerning aspect as cleft patients generally undergo multiple radiological examinations throughout their lifetime, which can lead to increased radiation exposure (55).

Dynamic magnetic resonance imaging (MRI) has been introduced to overcome the aforementioned obstacles as a non-invasive, non-ionizing imaging modality (88). Technological advancements enabled the visualization of the velopharyngeal muscle morphology and function. Even though the image quality of videofluoroscopy is considered superior (89, 90), dynamic MRI can be considered as an alternative imaging

modality for the diagnosis of VPI. The main burden of its application is the limited access due to its high costs.

To our knowledge, there are no existing studies on the application of dynamic CBCT imaging for the diagnosis of velopharyngeal insufficiency in patients with clefts.

DOI:10.14753/SE.2025.3097

2. Objectives

The overreaching purpose of this thesis was to improve patient care by investigating the application of Cone Beam CT imaging in orofacial cleft management.
Our aim was to provide knowledge and develop tools for further Cone Beam CT optimization studies in this field.
Additionally, the application of a novel tool for the diagnosis of VPI and a virtually assisted surgical technique for cleft surgery were evaluated.

This doctoral thesis was based on 4 research projects:

1. Determining the age and gender-specific maxillary dimensions of pediatric patients
2. Evaluation of a complex virtual planning method combined with 3D-printing in alveolar bone grafting
3. Development of age-specific pediatric phantom skulls with artificial orofacial clefts
4. Validation of Cone Beam CT imaging in the diagnosis of velopharyngeal insufficiency

3. Methods

3.1. Determining the age and gender-specific maxillary dimensions of pediatric patients

This retrospective study has been conducted with institutional ethical review board approval (UZ Leuven, reference number: S53225). Informed consent was obtained from all patients at the time of enrollment into the study database, in compliance with the World Medical Association Declaration of Helsinki on medical research.

The age groups have been defined from 8 to 20 years as this is the age range when cleft patients undergo alveolar bone grafting or other interventions related to the hard tissues (e.g. impacted teeth) and, accordingly, radiological imaging is carried out.

From a radiological aspect the different treatment phases include: planning of the secondary alveolar bone grafting (7-9 years), evaluation of the bone graft and canine eruption (10 years), evaluation and planning of orthognathic surgery (15 years) and final evaluation of the treatment (20 years) (59). Individual deviations may occur due to the growth alterations in cleft patients. The imaging modality of choice is most commonly Cone Beam CT.

The sample size was calculated using a priori power analysis in G*power 3.1 software (3.1.7 for Windows, Heinrich Heine, Universität Dusseldorf, Germany) at a power of 80% and 0.05 level of significance. Previous studies were used to determine the specific effect size for maxilla measurement (91).

Images were acquired using three different Cone Beam CT devices: Planmeca Promax 3D Max (Planmeca, Helsinki, Finland), 3D Acquitimo 170 (J Morita, Kyoto, Japan) and Newtom VGI Evo (Cefla, Imola, Italy). Image acquisition settings were standardized, following the recommendations of Stratis et al (70).

Patients were allocated into gender and age-specific groups. The inclusion criteria consisted of Caucasian patients between 8 and 20 years of age, who underwent CBCT scanning. To identify all landmarks, only scans with good image quality and large Field of Views were included (which covered the entire upper arch). Exclusion criteria were missing, restored, or impacted bilateral first molars/incisors, large metal restorations and

motion artifacts as these negatively impact image quality. As our objective was to define the maxillary dimensions of the normal patient population, subjects who underwent major maxillofacial surgeries or presented with congenital anomalies that influence craniofacial growth, were excluded (e.g. cleft lip and palate, hemifacial microstomia, and other syndromic conditions).

Maxillary dimensions were assessed by linear measurements in three planes: axial, coronal, and sagittal, based on anatomical landmarks. These were predefined based on previous publications evaluating maxillary growth or age-specific dimensions (92). Seven distance-based variables were evaluated: anterior nasal spine–posterior nasal spine (ANS-PNS) distance, bilateral maxillary first molar's central fossae (CF) distance, palatal vault depth (PVD), bilateral palatal cementoenamel junction (PCEJ) distance, bilateral vestibular cementoenamel junction (VCEJ) distance, bilateral jugular distance (Jug), and arch length (AL).

Images were retrieved from the PACS/AFGA picture archiving workstation (AFGA Gevaert Group, Mortsel, Belgium). After image reorientation, all linear measurements were carried out on 2D images in the integrated clinical workstation (KWS, UZ Leuven, Belgium). After calibration, measurements were performed (Figure 2.) by two trained observers with over 5 years of experience in oral radiology under the supervision of a maxillofacial radiologist on a Barco Dental Screen (MDRC-2222 Option WP, Barco NV, Kortrijk, Belgium). Disagreements related to landmark placement or measurements were solved by consensus.

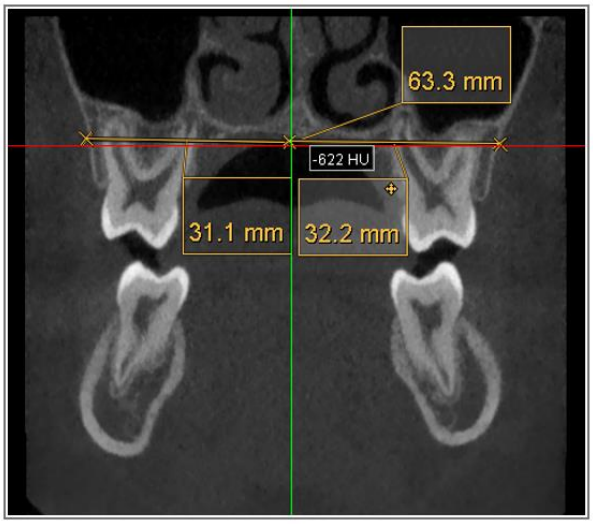

Figure 2. – Linear measurements of maxillary dimensions on CBCT (coronal view)

Statistical analysis was conducted in the SPSS software (version 12.0.1, SPSS Inc., Chicago, USA). The normality of data distribution was confirmed by applying the Kolmogorov-Smirnov test. The accuracy of landmark identification was elucidated through the coefficient of variation (CV) [CV = (standard deviation/mean) × 100%], which acted as an indicator of reproducibility by providing the precision error of measurements. A locally weighted scatterplot smoothing curve (LOWESS) was fit through the graphs showing the measured distances concerning age groups. Inter-gender differences were evaluated using independent t-tests, performed with statistical significance set at $p < .05$.

3.2. Evaluation of a complex virtual planning method combined with 3D-printing in alveolar bone grafting

This retrospective study was conducted with institutional ethical board approval. Data were analyzed of 28 cleft patients, who underwent surgical cleft repair at the Department of Pediatrics, Semmelweis University Budapest, between September 2017 and September 2020. A single surgeon (KN) performed the interventions following the same surgical protocol. Both unilateral (UCLP) and bilateral (BCLP) cleft lip and palate patients were included.

As a first step pre-operative clinical examination was carried out to verify the proper transverse relations of the maxillary segments to perform bone augmentation. If selected for alveolar bone grafting, patients underwent Cone Beam CT imaging (voxel size 0,3-0,4 mm). In some cases, multi-slice CT scans were used, if imaging was previously requested by other medical specialists.

Subsequently segmentation of the bony structures was performed in Slicer software (slicer.org) using preset threshold values. The same software served as a designing tool for the primary shape of the bone graft. This was accomplished by outlining the bone defect step-by-step, on the cross-sectional axial view of the CBCT scans. The resulting virtual shape was equivalent with the desired bone graft. The objects were exported in STL format (standard tessellation language).

After importing the objects, fine adjustments of the objects were carried out in Meshmixer software (Autodesk Inc., San Rafael, California, USA). This was important to achieve a smooth structure that allows good quality 3D printing. After establishing the form and dimensions of the bone graft, we followed the method of Fábián et al (93) to design the surgical mold (Figure 3). In an open-source computer-aided design CAD software (Blender, Blender Foundation, Amsterdam, the Netherlands) two overlapping cubes were designed. Subsequently, the previously designed bone graft was placed in the center and was virtually subtracted. This resulted two virtual cubes with a negative form of the bone graft.

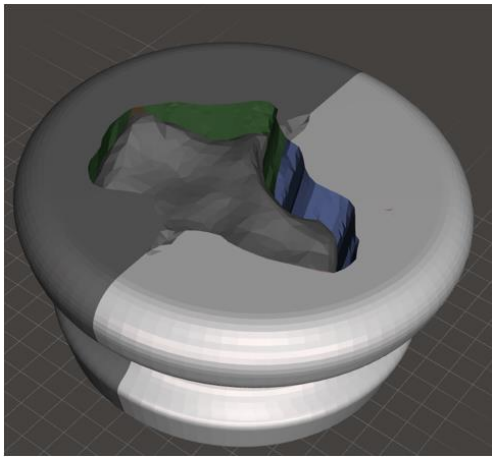

Figure 3. – Virtually designed surgical mold for alveolar bone grafting

The surgical molds were manufactured by 3D printing using an Objet Prime 3D printer (Stratasys, Rehotov, Israel) and Med610 resin (Stratasys, Rehotov, Israel). However after 2019 we used a Phrozen Shuffle XL 3D printer (Phrozen, Hsinchu City, Taiwan) with NextDental Dental SG resin (NextDent B.V., Soesterberg, The Netherlands), this did not alter the main concept. Both resins are classified as the highest Biocompatible Class I, sterilization was carried out in an autoclave. In the same manner, the virtual bone graft was printed as well, to serve as a visual reference during surgery.

Secondary alveolar grafting was carried out in general anesthesia. In a two-team approach cancellous bone, and bone chips were harvested using curettes from the iliac crest. Preparation of the alveolar cleft site and the iliac crest was performed simultaneously.

DOI:10.14753/SE.2025.3097

The collected bone was placed in the surgical molds and gently pressed to adapt to its form (Figure 4.). To increase the stability of the graft, fibrin glue was added (Tisseel 2ml, Baxter, Deerfield, USA). Subsequently, a collagen sponge was inserted into the donor site and the wound in the iliac region was closed in layers.

Before the preparation of the cleft site, local anesthesia was administered (Lidocaine with 0,2% Adrenaline). After the incision, full-thickness mucoperiosteal flaps were elevated. Eventual oronasal fistulas were closed before the graft insertion. Once the bone graft was positioned, the flaps were closed, aiming for tension-free closure. Postoperatively antibiotics were administered (amoxicillin 30mg/kg, or clindamycin 5 mg/kg every 8 hours).

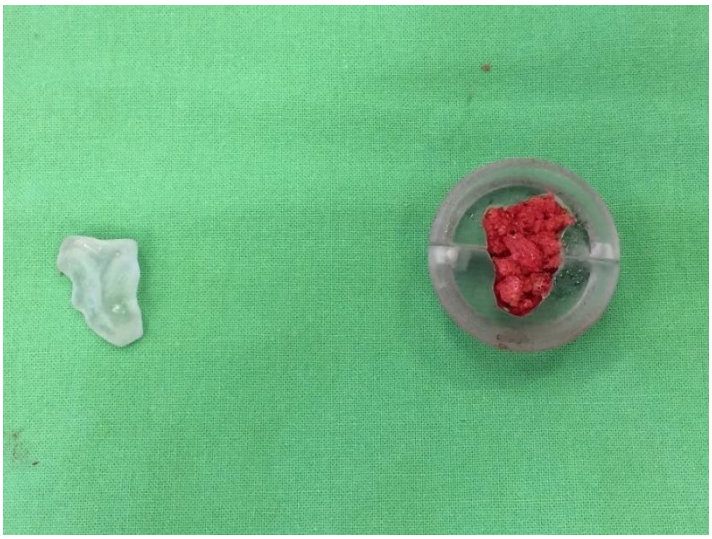

Figure 4. – The harvested autologous bone applied in the 3D printed individual mold

Following the surgery, we asked patients or their parents to fill out quality of life questionnaires to assess the patient's self-perception. A modified Health Related Quality of Life Measure (OHQoL) questionnaire was applied, it included 15 questions regarding healing, post-operative bleeding/swelling, medication, eating habits, weight changes, and overall satisfaction with the surgery. The follow-up period varied, the mean time between the intervention and the end of the survey was 17,41 months.

Statistical analysis was performed in R Studio 3.4.2. Collected data was presented as the mean standard error of the mean (SEM). Statistical analysis included the utilization of Fisher's exact probability test or a one-way analysis of variance (ANOVA) followed by Tukey's multiple comparison test for post hoc analysis. The p-value was less than 0.05 and therefore considered statistically significant.

3.3. Development of age-specific pediatric phantom skulls with artificial orofacial clefts

With institutional ethical approval (Semmelweis University, reference number: 265a/2019) six pediatric human skulls were obtained from the Hungarian Natural Museum (Budapest, Hungary). The age range of the skulls was 5-10 years. We chose this age group as usually this is the stage when patients undergo alveolar bone grafting and CBCT scans are taken.

Skulls with well-preserved anatomical structures were selected, based on their estimated anthropological age. Cone Beam CT scans (FOV: 12x8 cm, voxel size: 0,2mm, VGI Evo, New Tom, Verona, Italy) were carried out on all skulls to confirm the age and the integrity of hard tissues. Initial evaluation detected the presence of dental germs, missing teeth and mesiodens. None of the skulls contained large metal restorations or dental implants which could influence the image quality by scattering.

Images were exported in Digital Communications in Medicine format (DICOM) and imported to Mimics software (version 21, Materialise, Leuven, Belgium). Segmentation of bony structures was performed using preset threshold values based on image intensity. Subsequently, to reduce computing time, the region of interest (ROI) was cropped to the maxilla.

Following the segmentation of the upper arch and the surrounding bones, the artificial clefts were designed. All artificial defects were designed unilaterally and on the left side as this side is clinically more common (94).

As a first step we used the “multiple slice edit” function of the software. Starting from the nasal base, the outline of the artificial clefts was drawn step by step on every fifth frame of the scan, scrolling caudally. As a reference, several CBCT scans of clinical cases were evaluated as a visual guide. The result was a three-dimensional volume, in the shape

of the bony defect we aimed to create. Further refinement of the segmented structures was performed by using the “region grow”, “multiple slice edit” and “contour editing” functions of the software.

After the segmentation, the objects (segmented maxilla and artificial clefts) were exported in STL format (standard tessellation language) and imported to 3matic® surgical planning software (version 14, Materialise, Leuven, Belgium) for the design of the cutting guides. Clinically orofacial clefts present as a pyramid-like bony defect, in order to achieve this shape, we created two different cutting guides: a “frontal” and a “palatal” guide. By placing the two guides and sequentially cutting the bone from two directions, the remaining bone represented the appearance of a natural cleft.

Cutting guides were designed individually for each skull and manufactured by 3D printing. The frontal guides had a more complex design (Figure 5.), consisting of two wings, a base, and a connecting ring. The individual cutting guides we designed as follows: first, the two different surfaces (frontal and palatal) of the artificial cleft were marked in the software using the “mark brush” function. This corresponded to the area of the skull that we planned to remove with each guide. The cutting angles of the guide were set by the “create a line” function of the software. The direction has been defined by selecting two points in the three-dimensional space. The two walls of the cutting guide followed these directions thus determining the cutting angles. The base of the frontal and the palatal cutting guides were designed by applying the “extrusion”, “hollow”, “boolean subtraction” and “wrap” functions of the software. After the virtual planning, the guides were manufactured by a Polijet 3D printer (Objet30 Prime, Stratasys, Rehotov, Israel) using Med610 resin (Stratasys, Rehotov, Israel).

Before applying the cutting guides on the dry skulls, a plastic skull and corresponding cutting guides were manufactured by 3D printing (Objet30 Prime, Stratasys, Rehotov, Israel) using Med610 resin (Stratasys, Rehotov, Israel), to perform a pilot intervention. In this way all steps of the developed workflow were tested and verified for accuracy, before the osteotomies were performed on the dry skulls.

Creation of the artificial clefts on the pediatric dry skulls was carried out by an experienced maxillofacial surgeon using the previously manufactured guides, piezoelectric, and rotating surgical instruments. The cutting outline and angulation were verified visually (Figure 6).

DOI:10.14753/SE.2025.3097

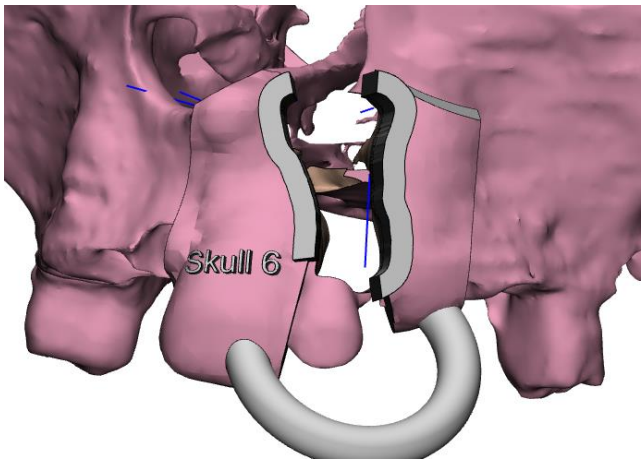

Figure 5. – Virtual planning of the osteotomy, frontal guide

Figure 6. – Precise fit of the individually created cutting guide on the dry skull

To mimic human soft tissue on the scans, all six pediatric skulls with artificial clefts were covered with Mix-D, a soft tissue equivalent material.

We followed Oenning et al in preparing the material (77), fractioned portions of Mix-D were created by mixing paraffin, polyethylene, magnesium oxide, and titanium oxide. To ensure chemical safety the preparation has been carried out under a fume hood. Prior to immersion in the material, larger foramina of the skulls (e.g. foramen magnum, orbita) and the interdental spaces were covered with crepe tape (paper with adhesive resin-

rubber-based, 24 mm width; 3M, Maplewood, USA) to avoid the material to enter in the intracranial region. The skulls were repeatedly immersed in melted Mix-D, adding material layer-by-layer to achieve a consistent thickness of the material. The mandibles were covered separately, and tongue models were created as well. After 24 hours of drying, larger irregularities and material excess on teeth and interdental areas were removed using wax carving instruments.

For the validation of the resulting radiological phantom skulls, CBCT scans were taken. Image acquisition was carried out with a high-resolution protocol (FOV: 12x8 cm, voxel size: 0,2mm, VGI Evo, New Tom, Verona, Italy). The evaluation was performed by two dentomaxillofacial radiologists who investigated the alignment, thickness, and uniformity of the material. The presence of eventual inhomogeneities, air bubbles, and artifacts was assessed. Only skulls properly mimicking human tissues were accepted.

The resulting pediatric phantom skulls with artificial clefts were denoted as “Dimicleft series” (Figure 7.).

Figure 7. - Dimicleft series: age-specific anthropomorphic radiological phantoms with artificial orofacial clefts

DOI:10.14753/SE.2025.3097

3.4. Validation of Cone Beam CT imaging in the diagnosis of velopharyngeal insufficiency

With institutional ethical review board approval (Semmelweis University, reference number: 265/2019) nine pediatric patients, between the age of 6 and 10 years, were enrolled in this study. The patient sample consisted of 3 surgically managed unilateral or bilateral cleft lip and palate (UCLP or BCLP) patients with VPI, 3 surgically managed unilateral cleft lip and palate (UCLP) or cleft palate (CP) patients without VPI, and 3 non-cleft patients as a control group.

Prior to imaging, all nine patients underwent speech evaluation by a speech therapist as a baseline diagnosis. Subsequently dynamic Cone Beam CT scanning was carried out, applying patient-specific exposure settings (based on tube current modulation). Three-dimensional imaging was justified for all three groups: pre-operative planning and orthodontic assessment for cleft patients and the evaluation of other dental deformities (e.g. mesiodens, impacted teeth) for the control group.

Image acquisition was carried out using the dynamic acquisition function of the Cone Beam CT machine (tube voltage: 110 kv, tube current: 3 mA, VGI Evo, New Tom, Verona, Italy). Imaging parameters were set at a default 20 frames per second.

During acquisition, patients were asked to perform speech tasks to evaluate their velopharyngeal function. The scans resulted in a series of two-dimensional images which were presented as a video to two observers.

After training and validation on the diagnostic criteria, subjective image quality assessment was carried out. The following anatomical landmarks were defined:

soft tissue outlines of the posterior pharyngeal wall and the soft palate. The main diagnostic task was to visualize velopharyngeal closure and to assess correlation with previous diagnosis based on speech evaluation (Figure 8. and 9.). Diagnostic agreement has been reached for all cases.

DOI:10.14753/SE.2025.3097

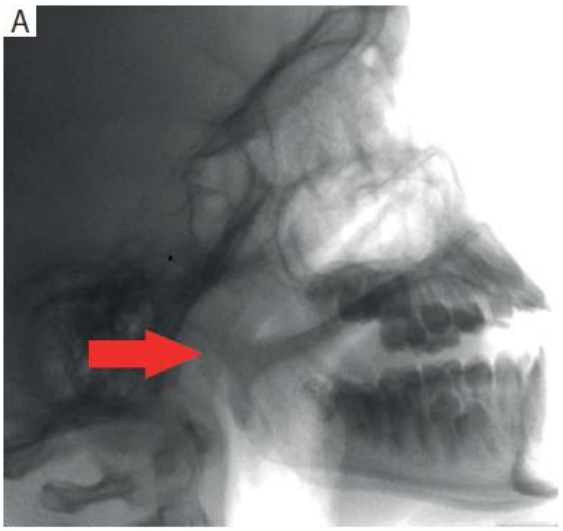

Figure 8. – Proper velopharyngeal closure in patient without VPI
(courtesy of Dr. Krisztián Nagy)

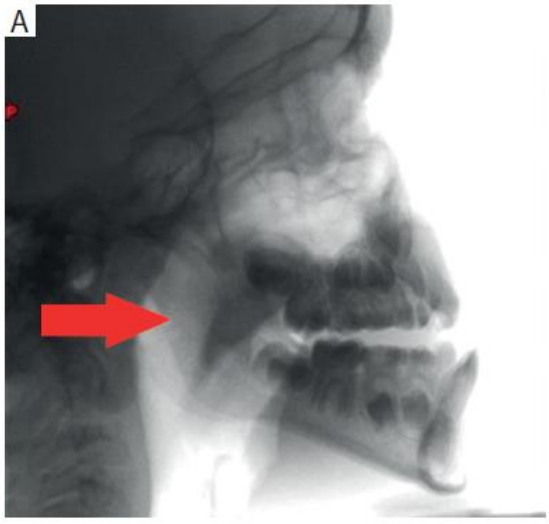

Figure 9. – Disrupted velopharyngeal movement in patient with VPI
(courtesy of Dr. Krisztián Nagy)

DOI:10.14753/SE.2025.3097

4. Results

4.1. Determining the age and gender-specific maxillary dimensions of pediatric patients

In total images of 1890 patients (892 male and 998 female) were assessed, from which 529 CBCT scans were selected based on the inclusion and exclusion criteria, resulting a balanced representation of both genders (243 male and 286 female). Patients were divided into different age groups, ranging from 8 to 20 years. The coefficient of variation (CV) values for all measurements were <5%, demonstrating a high level of reproducibility and consistency in landmark placement.

The descriptive statistics of mean linear maxillary dimensions showed different dimensions in all age groups (Table 2.). ANS-PNS and PVD showed the largest increase between 8 to 20 years of age. Arch length (AL) had the least variability in the different age groups. All measured values were within a 5 mm range of deviation. Age-specific groups showed larger dimensions for male patients for all measured structures. Curve analysis showed increasing linear measurements values from 8 to 20 years of age, except for arch length, which showed a nonsignificant decrease (p=.163) (Figure 10.).

Table 2. – Mean ± standard deviation of linear maxillary measurements (mm) in different age groups

Age	ANS-PNS	CF	PVD	PCEJ	VCEJ	Jug	AL
8	46,9 ± 2,7	43,6 ± 2,3	13,1 ± 1,4	30,5 ± 2,1	51,3 ± 2,6	56,3 ± 2,8	33,4 ± 1,9
9	47,7 ± 2,7	45,3 ± 2,6	13,6 ± 1,5	32,3 ± 2,9	53 ± 2,7	59,1 ± 2,6	32,7 ± 2,3

10	49,5 ± 2,8	46 ± 2,8	14,7 ± 1,9	33 ± 2,5	53,6 ± 2,9	59 ± 3,4	33,5 ± 2,6
11	50,2 ± 3,1	45,9 ± 3	14,5 ± 2,4	32,5 ± 2,8	53,5 ± 3,1	60,4 ± 4,6	32,7 ± 2,9
12	51 ± 3,8	45,9 ± 3,7	16,7 ± 2,4	33,2 ± 3,5	54,2 ± 3,5	61,48 ±4	33,1 ± 2,5
13	52 ± 3,1	46,5 ± 3	16,4 ± 2,3	33,8 ± 2,7	54,7 ± 3,5	63,3 ± 4,2	32,6 ± 2,5
14	53,2 ± 3	46,4 ± 3,5	17,8 ± 2,2	34,3 ± 3,2	55,2 ± 3,4	61,9 ± 4,5	32,9 ± 2,5
15	52,9 ± 2,8	46,6 ± 3,2	18,2 ± 2,1	33,5 ± 2,3	55,1 ± 2,5	62,4 ± 4,3	32,6 ± 2,6
16	53,8 ± 3,6	46,4 ± 3,4	19,2 ± 2,1	34 ± 2,9	55,2 ± 3,2	62,8 ± 4,8	32,5 ± 2,7
17	54,2 ± 4,2	47,7 ± 3,6	19 ± 2,4	34,4 ± 2,8	56,1 ± 3,4	63,1 ± 5,2	32,1 ± 1,8
18	54,6 ± 3,4	47,2 ± 2,8	20,1 ± 2,1	34,6 ± 2,8	56,2 ± 3,2	62,4 ± 4	31,7 ± 2
19	54,2 ± 4,2	46,4 ± 3,3	19,5 ± 2,1	34,4 ± 3,2	55,6 ± 3,8	63,7 ± 4,7	32,5 ± 1,6
20	53,5 ± 4	46,9 ± 3,3	20,3 ± 2,3	34,5 ± 2,9	55,6 ± 3,8	61,5 ± 4,7	31,8 ± 2,1

DOI:10.14753/SE.2025.3097

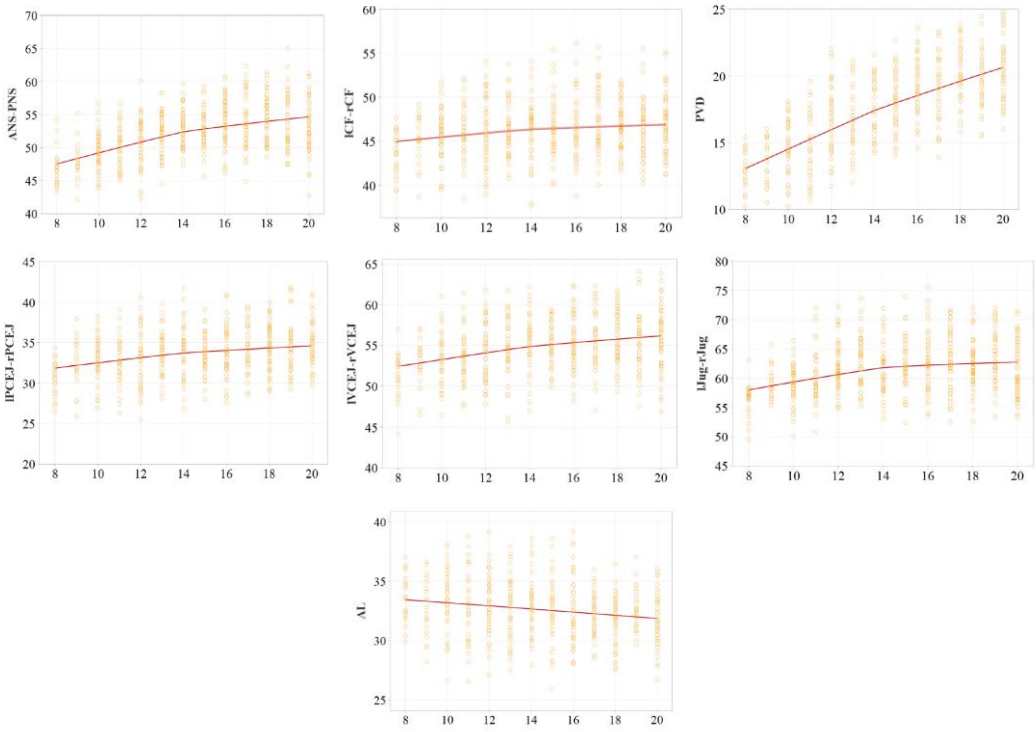

Figure 10. – Age-based locally weighted scatterplot smoothing curve of the seven distance-based variables, distances in millimeter.

4.2. Evaluation of a complex virtual planning method combined with 3D-printing in alveolar bone grafting

Data was analyzed from 28 cleft patients who underwent alveolar grafting procedures between September 2017 and September 2020.

15 male and 13 female individuals were enrolled in the study, the mean age of the patients was 16.96 ± 8.82 years (range: 10-49 years). Both unilateral (UCLP) and bilateral (BCLP) cleft lip and palate patients were included.

Analysis of the collected data showed that patients needed to take the prescribed antibiotics for at least 4 days (mean = 3.77 ± 1.73). No occurrences of bleeding in the oral cavity or the hip region were observed, and no reports of significant adverse effects were

reported. Following the surgery, facial swelling persisted for an average of 5 days (mean = 5 ± 1.52), and the wound on the hips impacted mobility for an average of 8 days (mean = 7.61 ± 3.64). Eighteen patients (69%) reported eating difficulties, while ten patients (38%) encountered weight loss after the surgery.

4.3. Development of age-specific pediatric phantom skulls with artificial orofacial clefts

Six pediatric phantom skulls with artificial unilateral clefts were developed.

Virtual planning of the cutting guides allowed the individual creation of each artificial cleft in the most realistic manner possible. All applied software, materials, and tools were accredited for clinical application. The workflow provided high accuracy and reliability; the 3D printed guides showed an accurate fit thus allowing precise guidance for the osteotomy.

Subsequently the skulls were covered in Mix-D, a soft tissue equivalent material.

Material infiltration of the nasal cavity, maxillary sinuses, and orbita resulted a realistic soft tissue thickness. The applied radio-opaque tape provided adequate protection for the larger apertures. Only small amounts of material entered the intracranial region through the foramen magnum, however the volume was minimal and outside of our field of interest. The alignment of the soft tissue equivalent material was sufficient, and no gaps between bony structures and material were detected. Evaluation of the resulting Cone Beam CT scans showed similar grey levels to soft tissues when compared with clinical images of pediatric cleft patients. No air bubbles, inhomogeneities, or artifacts in the soft tissue material could be detected.

Evaluations carried out by two maxillofacial radiologists verified that all pediatric phantom skulls appropriately mimicked the in vivo appearance of patients with unilateral clefts (Figure 11. and 12.).

DOI:10.14753/SE.2025.3097

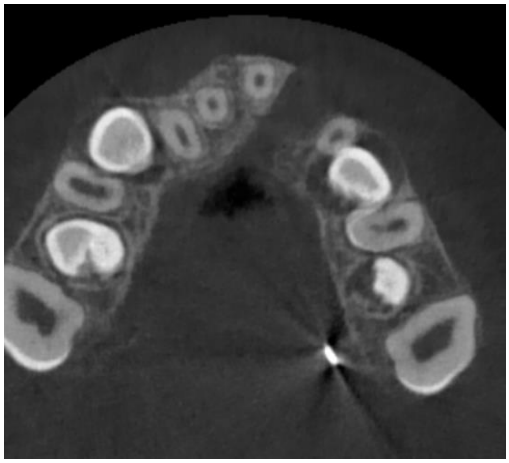

Figure 11. - Radiological appearance on CBCT image of a patient with cleft lip, palate, and alveolus (CLAP)

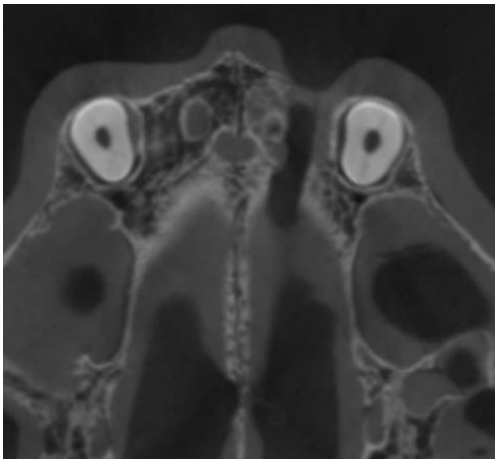

Figure 12. - Radiological appearance on CBCT of a radiological phantom skull with artificial cleft (Dimicleft series)

DOI:10.14753/SE.2025.3097

4.4. Validation of Cone Beam CT imaging in the diagnosis of velopharyngeal insufficiency

Nine pediatric patients underwent dynamic Cone Beam CT scanning. Patient-specific radiation doses varied individually due to automatic modulation of the device, based on anatomical characteristics of the patient, and ranged from 279 to 515 dose area product (DAP) (mGy x cm^2). Exposure time varied from 0,78-1,5 seconds and tube current value was set at the default value of 3 mA (milliampere). The resulting images were assessed by two observers, with the following findings: soft palate and posterior pharyngeal wall contour and movements were visible on all images. Both soft palate (dorso-caudal direction) and pharyngeal wall (ventro-caudal direction) movements were distinguishable on the images. Radiological assessment corresponded with prior speech test diagnosis as complete velopharyngeal closure could not be observed in the group of cleft patients with VPI. Additionally, a proportionally smaller dimension of the soft palate could be observed in all patients with cleft.

DOI:10.14753/SE.2025.3097

5. Discussion

5.1. Determining the age and gender-specific maxillary dimensions of pediatric patients

Previously established guidelines already emphasize the patient and indication-specific approach when it comes to CBCT acquisition in the pediatric population (41). Nevertheless, existing research findings are limited when concerning FOV optimization as part of patient specificity (69). Several studies have been conducted on CBCT optimization (both adult and pediatric patient populations), however, they primarily focused on other parameters than FOV (tube current, tube voltage, voxel size) (59) (62). Generally, CBCT devices offer only default options regarding FOV with a preset dimension of diameter and height (95). However, the possibility of dynamically adjusting FOV settings for each patient would allow the reduction of radiation dose without compromising the image quality of the scan. This personalized approach would allow optimization of the radiation exposure in delicate patient groups such as cleft patients. They generally undergo several radiological examinations during their lifetime, which can lead to increased radiation risk (55).

Existing studies on population-based pediatric maxillary dimensions have acquired data for diagnostic and treatment planning purposes. To our knowledge, no literature on normative, Cone Beam CT-based, skeletal measurements are available which could be implemented for pediatric Field of View (FOV) recommendations. Therefore, our study aimed to provide normative, age- and gender-specific data on pediatric maxillary dimensions.

The present study showed the dimensional changes of the upper arch size for different age groups between 8 and 20 years of age, in both genders. Scatterplot curves showed a gradual increase in maxillary dimensions in both genders, except for one linear measurement: the arch length (AL). It showed a decreasing trend, which deviation can be associated with the presence of diastema at a younger age, that in most cases closes during puberty (96). The collected data shows dissimilarities of measured dimensions in the

different age and gender groups. This emphasizes the importance of the current study and underlines the importance of individual FOV selection in the pediatric population instead of using default CBCT device settings (59).

Cone Beam CT optimization based on gender has not been documented yet. Our measurements suggest that male patients have significantly larger dimensions in all measured structures. This correlated with previously published studies which reported larger facial structures in boys (92). The presented data suggests, that despite the delayed growth spurt during puberty, boys have a longer period of active growth (65).

Additionally, current evidence also indicates that, in the long term, young females are more sensitive to radiation than male subjects, when receiving similar doses of radiation (97). This means a higher risk of cancer associated with radiation exposure for female patients (98) (99).

The presented normative values can serve as guidance for clinicians in gender-specific application of CBCT scans in children. However, CBCT devices already offer the option for dynamic FOV selection, there are currently still no studies on this topic. The acquired data could serve as orientation for CBCT manufacturers as well, to further adjust FOV sizes and include more options, corresponding to each age group and indication. Additionally, radiation doses can be further reduced by the application of automated algorithms (100).

Values provided by this current study confirmed the different maxillary dimensions in the age- and gender-specific pediatric patient groups. This underlines the need for further research in this field, investigating patients-specific FOV as a factor in radiation exposure. Limitations of the study include that only Caucasian patients were enrolled; therefore interpretation to other ethnic groups is limited. Nevertheless, the provided measurements can serve as a reference database, while other patient groups need to be further assessed to achieve a more sophisticated protocol.

Secondly, the normative data obtained from our measurements provided dimensions of pediatric patients with no conditions that alter the growth of the craniofacial structures. This dataset can serve as a baseline when comparing individuals with disturbed growth patterns such as orofacial cleft patients. As cleft patients reportedly present with collapsed maxillary arches, we hypothesize that the measurement values will be smaller in that

patient group. However further research needs to be carried out to provide the exact dimensions.

Additional limitations of the study include that the measurements were carried out exclusively on the maxillary arch. Therefore, the clinical application is reserved to conditions of this anatomical region. General recommendations for pediatric Cone Beam CT scanning cannot be formulated. Further investigations regarding the dimensions of the hard and soft tissues of the complete head and neck region should be performed.

5.2. Evaluation of a complex virtual planning method combined with 3D-printing in alveolar bone grafting

Orofacial cleft defects can present in various shapes and sizes. Therefore, aforementioned presurgical three-dimensional imaging of the bony structures has utmost importance. In combination with virtual planning, it provides the possibility to perform the intervention more accurately and predictably. The precise measuring of the cleft extent and the possibility of visualizing the anatomical structures in the region provides vital information to the operating surgeon.

There are many forms of Patient Related Outcomes that provide information about therapy results from a patient's perspective. For instance, quality-of-life questionnaires are well accepted for the evaluation of medical interventions (101). In craniofacial surgery the most frequently applied questionnaires are the Oral Health Impact Profile (OHIP-14), UK Health Related Quality of Life Measure (OHQoL-U), and Social Avoidance and Distress Scale (SADS) (102). In our study a modified OHQoL was used to evaluate the outcomes of the described virtually assisted surgical technique, focusing on the healing of the donor and cleft site. In our opinion, it is important to assess an operation technique not only from the aspect of the medical team but also from the angle of the patient.

The results of our study suggests a good acceptance from patiens and straightforward operation technique .

Limitations of the study included the wide range of ages, and the absence of a control group. In this regard patient number is a challenging question as orofacial clefts are a relatively rare condition.

5.3. Development of age-specific pediatric phantom skulls with artificial orofacial clefts

Radiation safety has become a pressing issue in cleft care, especially as the majority of patients are children, who are more sensitive to radiation risks. They generally undergo multiple scans throughout their lifetime (103), thus three-dimensional imaging has to be indicated with caution. Imaging optimization studies in the pediatric field have been limited by ethical concerns, as it not acceptable to perform in vivo studies only for optimization purposes.

For this task radiological phantoms are needed, which enable multiple image acquisitions of the same subject. Commercially available phantoms do not fulfill all needed requirements. Anthropomorphic pediatric phantom skulls were created by Oenning et al (DIMITRA series), but without clefts (77). However, we believe that it is crucial to include cleft defects in the image, as it highly impacts the radiation attenuation and scattering. This can influence voxel gray values in the region. To our knowledge, currently no age-specific radiological phantoms with unilateral clefts exist.

The described virtual planning protocol was proven to be a useful and precise tool for the creation of artificial clefts. Software and devices that are normally applied to reconstruct the integrity of the alveolar arch were used in a reverse, novel way. The described workflow can be integrated into similar research projects in which a predictable osteotomy on human dry skulls has to be performed.

The Mix-D preparation and application protocol that we followed was found reproducible and predictable. The importance of following the preparation recipe and sequence has been emphasized in other publications as well (77) (78), nevertheless Mix-D showed optimal radiological appearance due to its similar radiation attenuation characteristics.

The greatest difficulty remains the handling of the material, as it is applied in a melted form. To have precise control of the thickness of the material during embedding is challenging. Entering of the material through the larger cavities can be minimalized using non-radiopaque tape. In some cases, excessive material could be beneficial e.g. mimicking pathologies such as maxillary sinusitis. However, it is doubtful if such an exact application of the material would be possible. Another challenge is the rigid characteristic of the material after drying. It hinders the insertion of any dosimetric measurement tools,

which would provide more precise information on the effective dose of the scans in the different regions (77).

Limitations of the study include the absence of motion artefacts which is a common challenge in everyday clinical practice. Especially when cleft patients present with syndromic disorders or mental disabilities, cooperation of the patient can be very difficult. Secondly, even if the artificial cleft has been designed by following clinical images as a reference, the unsymmetric growth pattern of upper arches in cleft patients could not be achieved. Lastly, the soft and hard tissues of the neck e.g. were not included in the scans, as the Museum could not provide the matching cervical vertebrae of the skulls. This could have positively influenced image quality as it led to lower radiation attenuation by the structures in the anterior-posterior and posterior-anterior projection angles.

5.4. Validation of Cone Beam CT imaging in the diagnosis of velopharyngeal insufficiency

The assessment of velopharyngeal function has a high importance in the treatment of patients with clefts as irregular development of the structures often results in dysfunction. Various imaging techniques exist to evaluate VPI function in pediatric patients: flexible nasopharyngoscopy, videoflouroscopy or multiview fluoroscopy and dynamic magnetic resonance imaging (MRI). All the aforementioned imaging modalities allow the visualization and functional assessment of the velopharyngeal muscles, however, they have limitations. Applications can be constrained by low patient acceptance (flexible nasopharyngoscopy), radiation exposure (videoflouroscopy, multiview fluoroscopy) or limited access due to high scanning costs (MRI).

Cone Beam CT imaging is already an integrated tool in the management of patients with orofacial clefts. It serves as an essential modality for visualizing hard tissues in the pre-operative assessment and follow-up. Recently introduced developments of CBCT devices allow a novel type of image acquisition: a series of two-dimensional images in lateral or frontal view (dynamic CBCT scanning).

In our study we applied this new function to investigate the velopharyngeal structures.

All nine enrolled patients underwent speech evaluation prior to scanning. The main research question was if the diagnosis of the two assessment methods correlated.

Two observers rated the images according to pre-agreed criteria. Findings were in accordance with prior diagnosis: in the group of cleft patients with VPI a disrupted velopharyngeal function could be observed. Movements of the velopharyngeal structures such as soft palate, pharyngeal wall and the tongue were clearly distinguishable. Patients accepted well the image acquisition procedure as it was non-invasive and fast.

However, the application of Cone Beam CT imaging continues to raise issues regarding radiation exposure; in our study radiation dose was optimized by automated algorithms based on the individual anatomy of the patient.

The limitations of the study included the small sample of patients. Therefore, to verify our findings, further studies should be carried out involving a higher number of patients and other diagnostic tasks.

DOI:10.14753/SE.2025.3097

6. Conclusions

Overall, the described projects, despite their limitations, fulfilled the desired overreaching aim to further develop the application of Cone Beam CT imaging in cleft care.

6.1. Determining the age and gender-specific maxillary dimensions of pediatric patients

Our study provided a normative dataset of pediatric patients between 8 and 20 years of age. The findings underlined the importance of patient specific image acquisition as dimensions significantly varied among the different age and gender groups.
The data can be integrated into age- and gender specific recommendations for pediatric Cone Beam CT imaging. Field of View settings can be further adjusted for different indications such as diagnostic, surgical planning, and follow-up imaging purposes.

6.2. Evaluation of a complex virtual planning method combined with 3D-printing in alveolar bone grafting

The presented workflow developed in our center included virtual surgical planning and the fabrication of individual surgical molds. In our experience, it resulted in a more accurate and predictable operation technique. The visualization and guidance provided by the methods allowed the operating surgeon more confidence during the operation. Patient-reported outcomes confirmed good patient acceptance and no further burden to hospitalization.

DOI:10.14753/SE.2025.3097

6.3. Development of age-specific pediatric phantom skulls with artificial orofacial clefts

The developed Dimicleft phantom collection has been validated to appear in a real-life matter on radiological images, thus can be used for further optimization studies in this field. In our opinion, currently this approach is providing the most realistic appearance on radiological images. The phantoms can be used to perform further research can be performed to access different acquisition parameters or the performance of different CBCT units for the same specific diagnostic task. In particular, low-dose scanning protocols could be further investigated as image quality and radiation dose are in a sensitive balance. Various clinical tasks, such as diagnosis and segmentation related to virtual planning or follow-up can be evaluated objectively. Moreover, indication specific protocols can be established for different CBCT devices.
The Dimicleft phantom series can be used for further studies for the optimization of Cone Beam CT scanning in pediatric patients with clefts.

6.4. Validation of Cone Beam CT imaging in the diagnosis of velopharyngeal insufficiency

In the described study we assessed a novel function of a specific Cone Beam CT device to investigate the velopharyngeal function. Our findings suggest that the modality can provide clinically relevant images and could potentially become an alternative to other diagnostic modalities evaluating VPI.

DOI:10.14753/SE.2025.3097

7. Summary

Patients with orofacial clefts present with complex hard and soft tissue deficiencies. Incomplete development can result in esthetic and functional problems, such as the presence of oronasal fistula, collapsed maxillary dimensions, facial asymmetry, malocclusion, and speech disorders.

The management of the defect is carried out in a team approach, involving oral surgeons, orthodontists, plastic surgeons, and speech therapists. In general patients undergo multiple interventions, from already early childhood on.

Clinical imaging has utmost importance in the diagnostic and pre-operative workflow, thus radiological examinations are carried out more often in cleft patients compared to the non-cleft patient population. This results in an increased radiological exposure and associated risk for patients with cleft, especially as most patients are children.

Recently Cone Beam CT imaging has become the modality of choice for the evaluation of cleft patients. It provides three-dimensional images of bony structures with sufficient image quality and relatively low radiation dose. Nevertheless radiation safety remains a pressing issue.

The aim of the projects included in this thesis was to investigate Cone Beam CT imaging and provide knowledge and tools for further research on imaging optimization related to cleft care.

Findings of our study provided pediatric maxillary dimensions, which data can be applied in further Field of View optimization studies.

With the development of radiological phantoms with clefts we created a tool for testing different CBCT imaging protocols and achieve optimization for specific indications.

Additionally, the application of CBCT in the surgical planning of alveolar bone grafts and in the diagnosis of VPI represent further justification of this imaging modality.

8. References

1. Global strategies to reduce the health care burden of craniofacial anomalies: report of WHO meetings on international collaborative research on craniofacial anomalies. Cleft Palate Craniofac J. 2004;41(3):238-43.
2. Leslie EJ, Marazita ML. Genetics of cleft lip and cleft palate. Am J Med Genet C Semin Med Genet. 2013;163C(4):246-58.
3. Allori AC, Mulliken JB, Meara JG, Shusterman S, Marcus JR. Classification of Cleft Lip/Palate: Then and Now. Cleft Palate Craniofac J. 2017;54(2):175-88.
4. Waite PD, Waite DE. Bone grafting for the alveolar cleft defect. Semin Orthod. 1996;2(3):192-6.
5. Cho-Lee GY, García-Díez EM, Nunes RA, Martí-Pagès C, Sieira-Gil R, Rivera-Baró A. Review of secondary alveolar cleft repair. Ann Maxillofac Surg. 2013;3(1):46-50.
6. Le BT, Woo I. Alveolar cleft repair in adults using guided bone regeneration with mineralized allograft for dental implant site development: a report of 2 cases. J Oral Maxillofac Surg. 2009;67(8):1716-22.
7. Swanson JW, Yao CA, Auslander A, Wipfli H, Nguyen TH, Hatcher K, et al. Patient Barriers to Accessing Surgical Cleft Care in Vietnam: A Multi-site, Cross-Sectional Outcomes Study. World J Surg. 2017;41(6):1435-46.
8. Weissler EH, Paine KM, Ahmed MK, Taub PJ. Alveolar Bone Grafting and Cleft Lip and Palate: A Review. Plast Reconstr Surg. 2016;138(6):1287-95.
9. Solis A, Figueroa AA, Cohen M, Polley JW, Evans CA. Maxillary dental development in complete unilateral alveolar clefts. Cleft Palate Craniofac J. 1998;35(4):320-8.
10. Guo J, Li C, Zhang Q, Wu G, Deacon SA, Chen J, et al. Secondary bone grafting for alveolar cleft in children with cleft lip or cleft lip and palate. Cochrane Database Syst Rev. 2011(6):CD008050.
11. Janssen NG, Weijs WL, Koole R, Rosenberg AJ, Meijer GJ. Tissue engineering strategies for alveolar cleft reconstruction: a systematic review of the literature. Clin Oral Investig. 2014;18(1):219-26.
12. Papadopoulos MA, Koumpridou EN, Vakalis ML, Papageorgiou SN. Effectiveness of pre-surgical infant orthopedic treatment for cleft lip and palate patients: a systematic review and meta-analysis. Orthod Craniofac Res. 2012;15(4):207-36.
13. Thornton JB, Nimer S, Howard PS. The incidence, classification, etiology, and embryology of oral clefts. Semin Orthod. 1996;2(3):162-8.
14. Boyne PJ, Sands NR. Secondary bone grafting of residual alveolar and palatal clefts. J Oral Surg. 1972;30(2):87-92.
15. Schuchardt K. Modern trends in plastic surgery. Congenital deformities. I. Primary bone graft in clefts of lip, alveolus and palate. Mod Trends Plast Surg. 1966;2:214-25.
16. Ochs MW. Alveolar cleft bone grafting (Part II): Secondary bone grafting. J Oral Maxillofac Surg. 1996;54(1):83-8.

17. Lilja J. Alveolar bone grafting. Indian J Plast Surg. 2009;42 Suppl(Suppl):S110-5.
18. Slator R, Perisanidou LI, Waylen A, Sandy J, Ness A, Wills AK. Range and timing of surgery, and surgical sequences used, in primary repair of complete unilateral cleft lip and palate: The Cleft Care UK study. Orthod Craniofac Res. 2020;23(2):166-73.
19. Shaw WC, Semb G, Nelson P, Brattstrom V, Molsted K, Prahl-Andersen B, et al. The Eurocleft project 1996-2000: overview. J Craniomaxillofac Surg. 2001;29(3):131-40; discussion 41-2.
20. Fahradyan A, Tsuha M, Wolfswinkel EM, Mitchell KS, Hammoudeh JA, Magee W, 3rd. Optimal Timing of Secondary Alveolar Bone Grafting: A Literature Review. J Oral Maxillofac Surg. 2019;77(4):843-9.
21. Kim J, Jeong W. Secondary bone grafting for alveolar clefts: surgical timing, graft materials, and evaluation methods. Arch Craniofac Surg. 2022;23(2):53-8.
22. Grayson BH, Santiago PE, Brecht LE, Cutting CB. Presurgical nasoalveolar molding in infants with cleft lip and palate. Cleft Palate Craniofac J. 1999;36(6):486-98.
23. Millard DR, Jr., Latham RA. Improved primary surgical and dental treatment of clefts. Plast Reconstr Surg. 1990;86(5):856-71.
24. Nagy K, Mommaerts MY. Lip adhesion revisited: A technical note with review of literature. Indian J Plast Surg. 2009;42(2):204-12.
25. Palhazi P, Nemes B, Swennen G, Nagy K. Three-dimensional simulation of the nasoalveolar cleft defect. Cleft Palate Craniofac J. 2014;51(5):593-6.
26. Kaura AS, Srinivasa DR, Kasten SJ. Optimal Timing of Alveolar Cleft Bone Grafting for Maxillary Clefts in the Cleft Palate Population. J Craniofac Surg. 2018;29(6):1551-7.
27. Kyung H, Kang N. Management of Alveolar Cleft. Arch Craniofac Surg. 2015;16(2):49-52.
28. Pickrell K, Quinn G, Massengill R. Primary bone grafting of the maxilla in clefts of the lip and palate: a four year study. Plast Reconstr Surg. 1968;41(5):438-43.
29. Dempf R, Teltzrow T, Kramer FJ, Hausamen JE. Alveolar bone grafting in patients with complete clefts: a comparative study between secondary and tertiary bone grafting. Cleft Palate Craniofac J. 2002;39(1):18-25.
30. Hynes PJ, Earley MJ. Assessment of secondary alveolar bone grafting using a modification of the Bergland grading system. Br J Plast Surg. 2003;56(7):630-6.
31. Chang HP, Chuang MC, Yang YH, Liu PH, Chang CH, Cheng CF, et al. Maxillofacial growth in children with unilateral cleft lip and palate following secondary alveolar bone grafting: an interim evaluation. Plast Reconstr Surg. 2005;115(3):687-95.
32. Semb G. Effect of alveolar bone grafting on maxillary growth in unilateral cleft lip and palate patients. Cleft Palate J. 1988;25(3):288-95.
33. Kang NH. Current Methods for the Treatment of Alveolar Cleft. Arch Plast Surg. 2017;44(3):188-93.
34. Rawashdeh MA, Telfah H. Secondary alveolar bone grafting: the dilemma of donor site selection and morbidity. Br J Oral Maxillofac Surg. 2008;46(8):665-70.
35. Behnia H, Khojasteh A, Soleimani M, Tehranchi A, Atashi A. Repair of alveolar cleft defect with mesenchymal stem cells and platelet derived growth factors: a preliminary report. J Craniomaxillofac Surg. 2012;40(1):2-7.
36. Molnár B, Würsching T, Sólyom E, Pálvölgyi L, Radóczy-Drajkó Z, Palkovics D, et al. Alveolar cleft reconstruction utilizing a particulate autogenous tooth graft and a

novel split-thickness papilla curtain flap - A retrospective study. J Craniomaxillofac Surg. 2023.
37. Rudnick EF, Sie KC. Velopharyngeal insufficiency: current concepts in diagnosis and management. Curr Opin Otolaryngol Head Neck Surg. 2008;16(6):530-5.
38. Bergland O, Semb G, Abyholm FE. Elimination of the residual alveolar cleft by secondary bone grafting and subsequent orthodontic treatment. Cleft Palate J. 1986;23(3):175-205.
39. Kindelan JD, Nashed RR, Bromige MR. Radiographic assessment of secondary autogenous alveolar bone grafting in cleft lip and palate patients. Cleft Palate Craniofac J. 1997;34(3):195-8.
40. Witherow H, Cox S, Jones E, Carr R, Waterhouse N. A new scale to assess radiographic success of secondary alveolar bone grafts. Cleft Palate Craniofac J. 2002;39(3):255-60.
41. Oenning AC, Jacobs R, Pauwels R, Stratis A, Hedesiu M, Salmon B, et al. Cone-beam CT in paediatric dentistry: DIMITRA project position statement. Pediatr Radiol. 2018;48(3):308-16.
42. Scarfe WC, Farman AG, Sukovic P. Clinical applications of cone-beam computed tomography in dental practice. J Can Dent Assoc. 2006;72(1):75-80.
43. Quirynen M, Lamoral Y, Dekeyser C, Peene P, van Steenberghe D, Bonte J, et al. CT scan standard reconstruction technique for reliable jaw bone volume determination. Int J Oral Maxillofac Implants. 1990;5(4):384-9.
44. Jain S, Choudhary K, Nagi R, Shukla S, Kaur N, Grover D. New evolution of cone-beam computed tomography in dentistry: Combining digital technologies. Imaging Sci Dent. 2019;49(3):179-90.
45. Ludlow JB, Ivanovic M. Comparative dosimetry of dental CBCT devices and 64-slice CT for oral and maxillofacial radiology. Oral Surg Oral Med Oral Pathol Oral Radiol Endod. 2008;106(1):106-14.
46. Hamada Y, Kondoh T, Noguchi K, Iino M, Isono H, Ishii H, et al. Application of limited cone beam computed tomography to clinical assessment of alveolar bone grafting: a preliminary report. Cleft Palate Craniofac J. 2005;42(2):128-37.
47. Nemtoi A, Czink C, Haba D, Gahleitner A. Cone beam CT: a current overview of devices. Dentomaxillofac Radiol. 2013;42(8):20120443.
48. Choi HS, Choi HG, Kim SH, Park HJ, Shin DH, Jo DI, et al. Influence of the Alveolar Cleft Type on Preoperative Estimation Using 3D CT Assessment for Alveolar Cleft. Arch Plast Surg. 2012;39(5):477-82.
49. Spin-Neto R, Marcantonio E, Jr., Gotfredsen E, Wenzel A. Exploring CBCT-based DICOM files. A systematic review on the properties of images used to evaluate maxillofacial bone grafts. J Digit Imaging. 2011;24(6):959-66.
50. Oberoi S, Chigurupati R, Gill P, Hoffman WY, Vargervik K. Volumetric assessment of secondary alveolar bone grafting using cone beam computed tomography. Cleft Palate Craniofac J. 2009;46(5):503-11.
51. Shirota T, Kurabayashi H, Ogura H, Seki K, Maki K, Shintani S. Analysis of bone volume using computer simulation system for secondary bone graft in alveolar cleft. Int J Oral Maxillofac Surg. 2010;39(9):904-8.
52. Zhang W, Shen G, Wang X, Yu H, Fan L. Evaluation of alveolar bone grafting using limited cone beam computed tomography. Oral Surg Oral Med Oral Pathol Oral Radiol. 2012;113(4):542-8.

53. Linderup BW, Küseler A, Jensen J, Cattaneo PM. A novel semiautomatic technique for volumetric assessment of the alveolar bone defect using cone beam computed tomography. Cleft Palate Craniofac J. 2015;52(3):e47-55.
54. Albuquerque MA, Gaia BF, Cavalcanti MG. Oral cleft volumetric assessment by 3D multislice computed tomographic images. Int J Oral Maxillofac Surg. 2011;40(11):1280-8.
55. Jacobs R, Pauwels R, Scarfe WC, De Cock C, Dula K, Willems G, et al. Pediatric cleft palate patients show a 3- to 5-fold increase in cumulative radiation exposure from dental radiology compared with an age- and gender-matched population: a retrospective cohort study. Clin Oral Investig. 2018;22(4):1783-93.
56. Pauwels R, Cockmartin L, Ivanauskaite D, Urboniene A, Gavala S, Donta C, et al. Estimating cancer risk from dental cone-beam CT exposures based on skin dosimetry. Phys Med Biol. 2014;59(14):3877-91.
57. Jaju PP, Jaju SP. Cone-beam computed tomography: Time to move from ALARA to ALADA. Imaging Sci Dent. 2015;45(4):263-5.
58. Bushberg JT. Eleventh annual Warren K. Sinclair keynote address-science, radiation protection and NCRP: building on the past, looking to the future. Health Phys. 2015;108(2):115-23.
59. De Mulder D, Cadenas de Llano-Perula M, Willems G, Jacobs R, Dormaar JT, Verdonck A. An optimized imaging protocol for orofacial cleft patients. Clin Exp Dent Res. 2018;4(5):152-7.
60. Pauwels R, Seynaeve L, Henriques JC, de Oliveira-Santos C, Souza PC, Westphalen FH, et al. Optimization of dental CBCT exposures through mAs reduction. Dentomaxillofac Radiol. 2015;44(9):20150108.
61. Brasil DM, Pauwels R, Coucke W, Haiter-Neto F, Jacobs R. Image quality optimization of narrow detector dental computed tomography for paediatric patients. Dentomaxillofac Radiol. 2019;48(5):20190032.
62. Oenning AA-O, Pauwels RA-O, Stratis A, De Faria Vasconcelos K, Tijskens E, De Grauwe AA-O, et al. Halve the dose while maintaining image quality in paediatric Cone Beam CT. Sci Rep. 2019(2045-2322 (Electronic)).
63. Hesby RM, Marshall SD, Dawson DV, Southard KA, Casko JS, Franciscus RG, et al. Transverse skeletal and dentoalveolar changes during growth. Am J Orthod Dentofacial Orthop. 2006;130(6):721-31.
64. Heikinheimo K, Nyström M, Heikinheimo T, Pirttiniemi P, Pirinen S. Dental arch width, overbite, and overjet in a Finnish population with normal occlusion between the ages of 7 and 32 years. Eur J Orthod. 2012;34(4):418-26.
65. Stahl de Castrillon F, Baccetti T, Franchi L, Grabowski R, Klink-Heckmann U, McNamara JA. Lateral cephalometric standards of Germans with normal occlusion from 6 to 17 years of age. J Orofac Orthop. 2013;74(3):236-56.
66. Bruggink R, Baan F, Kramer GJC, Maal TJJ, Kuijpers-Jagtman AM, Bergé SJ, et al. Three dimensional maxillary growth modeling in newborns. Clin Oral Investig. 2019;23(10):3705-12.
67. Stern S, Finke H, Strosinski M, Mueller-Hagedorn S, McNamara JA, Stahl F. Longitudinal changes in the dental arches and soft tissue profile of untreated subjects with normal occlusion. J Orofac Orthop. 2020;81(3):192-208.
68. Al-Taai N, Persson M, Ransjö M, Levring Jäghagen E, Fors R, Westerlund A. Craniofacial changes from 13 to 62 years of age. Eur J Orthod. 2022;44(5):556-65.

69. Gaêta-Araujo HA-O, Alzoubi T, Vasconcelos KA-O, Orhan KA-O, Pauwels RA-O, Casselman JA-O, et al. Cone beam computed tomography in dentomaxillofacial radiology: a two-decade overview. Dentomaxillofac Radiol. 2020(0250-832X (Print)).
70. Stratis A, Zhang G, Jacobs R, Bogaerts R, Bosmans H. The growing concern of radiation dose in paediatric dental and maxillofacial CBCT: an easy guide for daily practice. Eur Radiol. 2019;29(12):7009-18.
71. Nejaim Y, Silva AI, Brasil DM, Vasconcelos KF, Haiter Neto F, Boscolo FN. Efficacy of lead foil for reducing doses in the head and neck: a simulation study using digital intraoral systems. Dentomaxillofac Radiol. 2015;44(8):20150065.
72. Richards AG, Webber RL. Constructing phantom heads for radiation research. Oral Surg Oral Med Oral Pathol. 1963;16:683-90.
73. Cook JE, Cunningham JL. The assessment of fracture healing using dual x-ray absorptiometry: a feasibility study using phantoms. Phys Med Biol. 1995;40(1):119-36.
74. Kamburoglu K, Kolsuz E, Murat S, Eren H, Yüksel S, Paksoy CS. Assessment of buccal marginal alveolar peri-implant and periodontal defects using a cone beam CT system with and without the application of metal artefact reduction mode. Dentomaxillofac Radiol. 2013;42(8):20130176.
75. Bechara B, Alex McMahan C, Moore WS, Noujeim M, Teixeira FB, Geha H. Cone beam CT scans with and without artefact reduction in root fracture detection of endodontically treated teeth. Dentomaxillofac Radiol. 2013;42(5):20120245.
76. Vasconcelos KF, Codari M, Queiroz PM, Nicolielo LFP, Freitas DQ, Sforza C, et al. The performance of metal artifact reduction algorithms in cone beam computed tomography images considering the effects of materials, metal positions, and fields of view. Oral Surg Oral Med Oral Pathol Oral Radiol. 2019;127(1):71-6.
77. Oenning AC, Salmon B, Vasconcelos KF, Pinheiro Nicolielo LF, Lambrichts I, Sanderink G, et al. DIMITRA paediatric skull phantoms: development of age-specific paediatric models for dentomaxillofacial radiology research. Dentomaxillofac Radiol. 2018;47(3):20170285.
78. Brand JW, Kuba RK, Braunreiter TC. An improved head-and-neck phantom for radiation dosimetry. Oral Surg Oral Med Oral Pathol. 1989;67(3):338-46.
79. Lewis JR, Andreassen ML, Leeper HA, Macrae DL, Thomas J. Vocal characteristics of children with cleft lip/palate and associated velopharyngeal incompetence. J Otolaryngol. 1993;22(2):113-7.
80. Glade RS, Deal R. Diagnosis and Management of Velopharyngeal Dysfunction. Oral Maxillofac Surg Clin North Am. 2016;28(2):181-8.
81. Croft CB, Shprintzen RJ, Rakoff SJ. Patterns of velopharyngeal valving in normal and cleft palate subjects: a multi-view videofluoroscopic and nasendoscopic study. Laryngoscope. 1981;91(2):265-71.
82. Shprintzen RJ, Golding-Kushner KJ. Evaluation of velopharyngeal insufficiency. Otolaryngol Clin North Am. 1989;22(3):519-36.
83. Marsh JL. Management of velopharyngeal dysfunction: differential diagnosis for differential management. J Craniofac Surg. 2003;14(5):621-8; discussion 9.
84. Conley SF, Gosain AK, Marks SM, Larson DL. Identification and assessment of velopharyngeal inadequacy. Am J Otolaryngol. 1997;18(1):38-46.
85. Witt PD, Marsh JL, McFarland EG, Riski JE. The evolution of velopharyngeal imaging. Ann Plast Surg. 2000;45(6):665-73.

86. D'Antonio LL, Marsh JL, Province MA, Muntz HR, Phillips CJ. Reliability of flexible fiberoptic nasopharyngoscopy for evaluation of velopharyngeal function in a clinical population. Cleft Palate J. 1989;26(3):217-25; discussion 25.
87. Henningsson G, Isberg A. Comparison between multiview videofluoroscopy and nasendoscopy of velopharyngeal movements. Cleft Palate Craniofac J. 1991;28(4):413-7; discussion 7-8.
88. Wein BB, Drobnitzky M, Klajman S, Angerstein W. Evaluation of functional positions of tongue and soft palate with MR imaging: initial clinical results. J Magn Reson Imaging. 1991;1(3):381-3.
89. Perry JL, Sutton BP, Kuehn DP, Gamage JK. Using MRI for assessing velopharyngeal structures and function. Cleft Palate Craniofac J. 2014;51(4):476-85.
90. Arendt CT, Eichler K, Mack MG, Leithner D, Zhang S, Block KT, et al. Comparison of contrast-enhanced videofluoroscopy to unenhanced dynamic MRI in minor patients following surgical correction of velopharyngeal dysfunction. Eur Radiol. 2021;31(1):76-84.
91. Fernandes VM, Jorge PK, Carrara CF, Gomide MR, Machado MA, Oliveira TM. Three-dimensional digital evaluation of dental arches in infants with cleft lip and/or palate. Braz Dent J. 2015;26(3):297-302.
92. Ursi WJ, Trotman CA, McNamara JA, Jr., Behrents RG. Sexual dimorphism in normal craniofacial growth. Angle Orthod. 1993;63(1):47-56.
93. Fábián Z, Kádár K, Patonay L, Nagy K. Application of 3D Printed Biocompatible Plastic Surgical Template for the Reconstruction of a Nasoalveolar Cleft with Preoperative Volume Analysis. Materiale Plastice 2019;56:413-5. .
94. Pradip R Shetye (Editor) TLGE. Cleft and Craniofacial Orthodontics: Wiley-Blackwell; 2022. 848 p.
95. Hung K, Hui L, Yeung AWK, Scarfe WC, Bornstein MM. Image retake rates of cone beam computed tomography in a dental institution. Clin Oral Investig. 2020;24(12):4501-10.
96. Alves ACM, Janson G, McNamara JA, Jr., Lauris JRP, Garib DG. Maxillary expander with differential opening vs Hyrax expander: A randomized clinical trial. Am J Orthod Dentofacial Orthop. 2020;157(1):7-18.
97. Belmans N, Oenning AC, Salmon B, Baselet B, Tabury K, Lucas S, et al. Radiobiological risks following dentomaxillofacial imaging: should we be concerned? Dentomaxillofac Radiol. 2021;50(6):20210153.
98. Hedesiu M, Marcu M, Salmon B, Pauwels R, Oenning AC, Almasan O, et al. Irradiation provided by dental radiological procedures in a pediatric population. Eur J Radiol. 2018;103:112-7.
99. De Felice F, Di Carlo G, Saccucci M, Tombolini V, Polimeni A. Dental Cone Beam Computed Tomography in Children: Clinical Effectiveness and Cancer Risk due to Radiation Exposure. Oncology. 2019;96(4):173-8.
100. Brasil DM, Merken K, Binst J, Bosmans H, Haiter-Neto F, Jacobs R. Monitoring cone-beam CT radiation dose levels in a University Hospital. Dentomaxillofac Radiol. 2023;52(3):20220213.
101. Dohan Ehrenfest DM, Andia I, Zumstein MA, Zhang CQ, Pinto NR, Bielecki T. Classification of platelet concentrates (Platelet-Rich Plasma-PRP, Platelet-Rich Fibrin-PRF) for topical and infiltrative use in orthopedic and sports medicine: current consensus, clinical implications and perspectives. Muscles Ligaments Tendons J. 2014;4(1):3-9.

102. The World Health Organization Quality of Life assessment (WHOQOL): position paper from the World Health Organization. Soc Sci Med. 1995;41(10):1403-9.
103. White SC, Scarfe WC, Schulze RK, Lurie AG, Douglass JM, Farman AG, et al. The Image Gently in Dentistry campaign: promotion of responsible use of maxillofacial radiology in dentistry for children. Oral Surg Oral Med Oral Pathol Oral Radiol. 2014;118(3):257-61.

9. Bibliography of the candidate's publications

The thesis was based on the following peer-reviewed publications:

- Shujaat S, Kesztyűs A, Song D, Regnstrand T, Benchimol D, Nagy K, Jacobs R. Moving toward patient specificity for devising cone-beam computed tomography field-of-views: A normative maxillary skeletal dimensional analysis. Int J Paediatr Dent. 2023 Sep;33(5):477-486. doi: 10.1111/ipd.13089. Epub 2023 Jun 12. PMID: 37203232. (IF: 3,8)

- Kesztyűs A, Würsching T, Nemes B, Pálvölgyi L, Nagy K. Evaluation of 3D visualization, planning and printing techniques in alveolar cleft repair, and their effect on patients' burden. J Stomatol Oral Maxillofac Surg. 2022 Sep;123(4):484-489. doi: 10.1016/j.jormas.2021.10.007. Epub 2021 Oct 19. PMID: 34678495. (IF: 2,2 – shared first authorship)

- Pálvölgyi L, Kesztyűs A, Shujaat S, Jacobs R, Nagy K. Creation of Dimicleft radiological cleft phantom skulls using reversed virtual planning technique. Dentomaxillofac Radiol. 2023 Oct;52(7):20230121. doi: 10.1259/dmfr.20230121. Epub 2023 Jun 22. PMID: 37395648; PMCID: PMC10552124. (IF: 3,3)

- Kesztyűs A, Pálvölgyi L, Jacobs R, Nagy K. Assessment of post-operative velopharyngeal closure in cleft palate patients using cone-beam computed tomography: a pilot study. Journal of Stomatology. 2021;74(2):65-69. doi:10.5114/jos.2021.106501. (IF: NA)

DOI:10.14753/SE.2025.3097

10. Acknowledgements

I am very grateful to people who supported me during my journey:

To Dr. Krisztián Nagy, my supervisor and mentor – for the continuing guidance and support these long years.

To the OMFS-IMPATH research team – for the important professional input and inspiring environment.

To my family, especially my Mum – for the continuous support.

To my wife Fatime – who despite all the never-ending professional projects didn't change her mind.